Pol. J. Environ. Stud. Vol. 28, No. 4 (2019), 2571-2583
DOI: *10.15244/pjoes/86226* ONLINE PUBLICATION DATE: 2019-03-05

Original Research

Characterization and Optimization of Photocatalytic Activity of Sol Gel-Synthesized TiO_2 and Ag-doped TiO_2 through Degradation of Synthetic Textile Effluent by UV Lamp-Assisted Experimental Setup

Tayyaba Muhammad Akram[1,2]*, Nasir Ahmad[3], Irfan Ahmed Shaikh[1]

[1]College of Earth and Environmental Sciences, University of the Punjab, Lahore, Pakistan
[2]Department of Science Education (IER), University of the Punjab, Lahore, Pakistan
[3]Institute of Geology, University of the Punjab, Lahore, Pakistan

Received: 7 March 2017
Accepted: 4 March 2018

Abstract

The textile industry is one of the largest producers of harmful effluent, and this has become a serious threat to the environment when disposed of into water bodies, which may lead to high pollution risk – especially in developing countries. There are several treatment methods ranging from conventional to advanced for treating textile effluent before disposal in the environment. Photocatalytic oxidation (AOPs) is the most sophisticated process among all other advanced oxidation processes. In this study, TiO_2 and Ag-doped TiO2 were used for the photcatalytic degradation of synthetic textile effluent. TiO_2 and Ag-doped TiO_2 catalyst were synthesized through two routes of sol-gel method (M1 and M2 reported in our previous study) for mobilized and immobilized utilization purposes [1], and characterization of the catalysts was carried out through X-ray diffrectrometric analysis. XRD patterns showed that catalysts synthesized by both routs of sol-gel method were initially found in amorphous form as no peak appeared in an X-ray diffractrogram at 0ºC calcination (catalyst without calcinations), whereas with an increase of temperature the amorphous form of catalyst turned into crystalline. Results showed that TiO_2 synthesized by the sol-gel route showed anatase phase at 350ºC, and peaks kept growing until 550ºC. Furthermore, at 650-750ºC anatase and rutile co-exist, while in Ag-doped TiO_2, anatase appeared at 350-450ºC and at 550ºC anatase phase/silver co-existed, whereas at 650-750ºC anatse-silver-rutile co-existed. An X-ray diffractrogram showed that catalyst synthesized through the 2nd sol-gel route also possessed an amorphous nature at 350ºC and peaks of anatase phase of TiO_2 appeared at 450ºC and kept growing sharper as temperature increased from 450-750ºC, whereas anatase peaks detected at 350ºC in Ag-TiO_2, and anatase-silver co-existed at 450ºC and 550ºC. Hence, anatase disappeared

*e-mail: tmabpu@hotmail.com

and only silver metal peaks remained at 650-750°C. Degradation and decolorization results revealed that optimum photocatalytic activity was achieved by catalysts calcinated at 550ºC as 91.96% degradation (COD removal %) with Ag-doped TiO_2 immobilized catalyst, and 99.57% decolorization (colour removal percentage) was achieved with Ag-doped TiO_2 mobilized catalyst on 60 min treatment of synthetic textile effluent (Remazol red RGB: 10 ppm concentration, pH3). Results showed that Ag-doped TiO_2 developed anatase crystalline phase at 550ºC that favored degradation and decolourization. The order of catalyst calcination at 550°C with respect to degradation was found as Ag-TiO_2 (immobilized) > Ag-TiO_2 (mobilized) > TiO_2 (mobilized) > TiO_2 (immobilized) and decolourization found as Ag-TiO_2 (mobilized) >Ag-TiO_2(immobilised)> TiO_2 (immobilized) > TiO_2 (mobilized).

Keywords: TiO_2 photocatalysis, characterization of catalyst, photocatalytic activity of TiO_2 and Ag doped TiO_2

Introduction

The textile industry is one of the largest effluent-producing sectors. Textile effluent generally contains a huge amount of dyes and chemicals that are considered to be toxic, carcinogenic, and harmful for the environment when disposed of in water bodies [2-8]. Advanced oxidation processes (AOPs) have been proven to be very effective for removing organic and inorganic pollutants, color, COD, and toxicity from textile effluent [9, 10]. Among AOPs, heterogeneous TiO_2 photocatalysis is the most sophisticated technology for oxidation of dyes and textile wastewater [11-18]. Titanium dioxide occurs in nature in well-known minerals such as rutile (tetragonal), anatase (tetragonal), and brookite (orthorhombic). Each phase of catalysis exhibits different physical properties, which are determined by their structural, chemical, and optoelectronic properties, which means that catalytic activity strongly depends upon its size, crystallinity, and shape [19-24]. These properties are controlled by the preparation conditions of the catalyst such as calcination temperature, calcination time, pH of the medium, and concentration (ratio of titanium tetrabuta oxide, water, and solvent) [25-28]. It is a well-established fact that calcination time and concentration ratio have no significant effect on the catalyst synthesis, whereas pH and calcination temperatures of the medium play vital roles in the anatase, rutile, and brokite crystal phase transformation and controlling the size of the crystallite, which effects the efficiency of the catalyst in degradation and decolorization of the textile effluent [29-34]. Calcination is a common treatment used to improve the crystallinity of TiO_2 powders and it was found that phase transformation from amorphous to crystalline anatase occurred at temperatures above 350°C [35, 36]. Synthesis of the catalyst sees two simultaneous reactions (hydrolysis and condensation) taking place that affect the crystallite size and the formation of the crystal phase. These reactions are sensitive to pH of the reaction medium. Acidic pH is used to restrain hydrolysis, while alkali can accelerate hydrolysis during reaction. Acidic medium is favorable for the synthesis of small crystallite, more active sites, and the formation of the anatase phase [24, 37, 38]. The effect of pH on crystallite size is a well-established fact. When the pH value is below 7 the size of crystallites are almost small and remain constant, which means acidic medium restrains crystallite growth, whereas pH value beyond 7 indicates that a total alkali environment would enhance crystallite size growth, which reduces the active site of the catalyst that is not favorable for the efficient photocatalytic oxidation of the pollutant. Smaller crystallite size and high active sites results in higher efficiency in the photodecomposition of the pollutants [30, 39-41].

In this study, the main focus was to synthesis catalysts (TiO_2 and Ag-doped TiO_2) to calcinate at different temperatures, to characterize in order to determine crystalline phase and structure, and to evaluate photocatalytic activity (performance) by COD removal and colour removal percentages.

Material and Methods

Synthesis and Doping Process of the Catalysts

TiO_2 and Ag-doped TiO_2 catalyst was synthesized through two routes of sol-gel method M1 and M2 for mobilized and immobilized application, respectively (these routes are reported in our previous research paper [1]). The synthesis of the catalyst and doping process was carried out by following a modified sol-gel method and then calcinated at 350°C, 450°C, 550°C, 650°C, and 750°C [1]. Substrate was prepared and coating the thin film catalyst was carried out by standard slurry coating method [1, 42].

Material and Chemicals

Titanium tetraisopropaoxide (97%), acitic acid (99.7%), silver nitrate (99%), nitric acid, ethanol, deionized water, and dental material.

Equipment and Instrumentation

A magnetic stirrer (0-1400 rpm) for continuous mixing of the effluent, analytical balance (Sartorius, BL 210S), oven (maximum range 250ºC), furnace. Characterization of the catalyst calcinated at 350ºC, 450ºC, 550ºC, 650ºC, and 750ºC was carried out by a Rigaku X-ray powder diffractometer (D-maxIIA, Rigaku, Japan), photocatalytic degradation was carried out in a double-walled rectangular box reactor (double-walled horizontal glass reactor [1].

Methodology

In this study, pH of the medium was kept acidic at 2 during the synthesis of the catalyst, which is favorable for small crystal size by preventing hydrolysis that restrains large crystal growth. TiO_2 was used alone as well as being doped with Ag metal to reduce the gape of valance and conduction band, and also to control the electron-hole recombination rate. Catalysts were then calcinated at 350ºC, 450ºC, 550ºC, 650ºC, and 750ºC to obtain desired anatase phase of TiO_2 to improve the crystallinity in order to enhance performance of the catalysts [28, 35, 43-45]. Performance of the catalyst was evaluated by degradation (COD removal percentage) and decolorization (colour removal percentage) of synthetic textile effluent (Remazol red RGB dye containing 10 ppm concentration, pH3) through mobilized and immobilized TiO_2 and Ag-doped TiO_2 under UV (400W) irradiation for 60 mins. For this purpose we used a double-walled rectangular box reactor (double walled horizontal glass reactor) [1].

Results and Discussion

Characterization of the Catalysts

TiO_2 and Ag-doped TiO_2 catalysts were characterized by X-ray diffractrometer (D-maxIIA, Rigaku, Japan) for determining the effect of calcination temperature on catalyst properties, such as crystalline phase, structure/ lattice, crystal size (nm), percent crystal, and percent amorphous ratio of the catalysts [33, 46-48]. Fig. 1 through 4 show the patterns of X-ray diffraction of TiO_2 and Ag-doped TiO_2, and Tables 1 through 4 summarize the X-ray diffractromtric data.

Figs 1 and 2 show the patterns of X-ray diffraction of TiO_2 and Ag-doped TiO_2 (synthesized by M1 route of sol gel) used in mobilized applications. TiO_2 and Ag doped TiO_2 were coded as M1A and M1B (neither pulverized nor calcinated), respectively. Furthermore, M1A1 and M1B1 (pulverized but not calcinated), M1A2 and M1B2 (calcinated at 350ºC), M1A3 and M1B3 (calcinated at 450ºC), M1A4 and M1B4 (calcinated at 550ºC), M1A5 and M1B5 (calcinated at 650ºC), and M1A6 and M1B6 (calcinated at 750ºC). It appears from figures 1 and 2 that in catalyst M1A1 and M1B1 (pulverized but not calcinated) peaks corresponding to anatase are absent, which implies that pure and doped titania are in amorphous form and showed lowest catalytic performance (Fig. 5). Hence, titania catalyst (pure TiO_2 and Ag-doped TiO_2) were calcinated for obtaining desired anatase crystal structure having high photocatalytic activity [49]. Pure TiO_2 and Ag-doped TiO_2 catalysts coded as M1A2 and M1B2, M1A3 and M1B3, M1A4 and M1B4, M1A5 and M1B5, and M1A6 and M1B6 were calcinated at 350ºC, 450ºC, 550ºC, 650ºC, and 750ºC, respectively.

Figs 1-4 demonstrated that diffraction peaks appearing at 2θ value correspond to the crystal phase of the catalyst (TiO_2 and Ag-doped TiO_2). The peaks

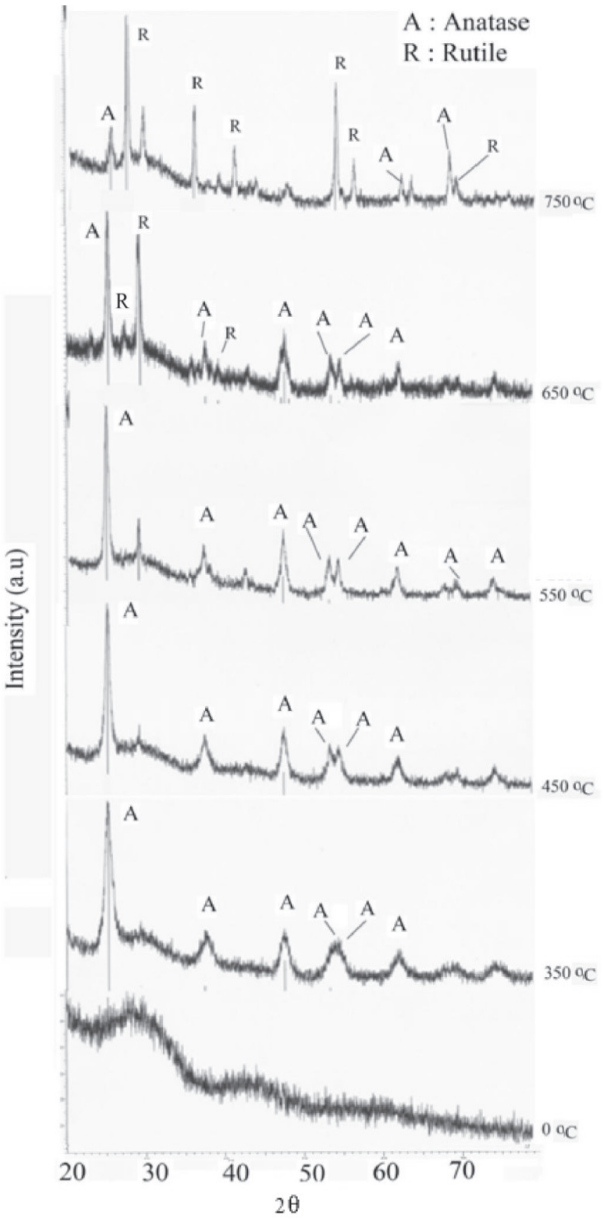

Fig. 1. X-ray diffractrograms of TiO_2 catalyst: 0ºC (without calcination), catalyst calcinated at 350ºC, 450ºC, 550ºC, 650ºC and 750 °C temperatures (TiO_2 catalyst synthesized through Ist sol gel route and used as mobilized form, A = anatase, R = rutile).

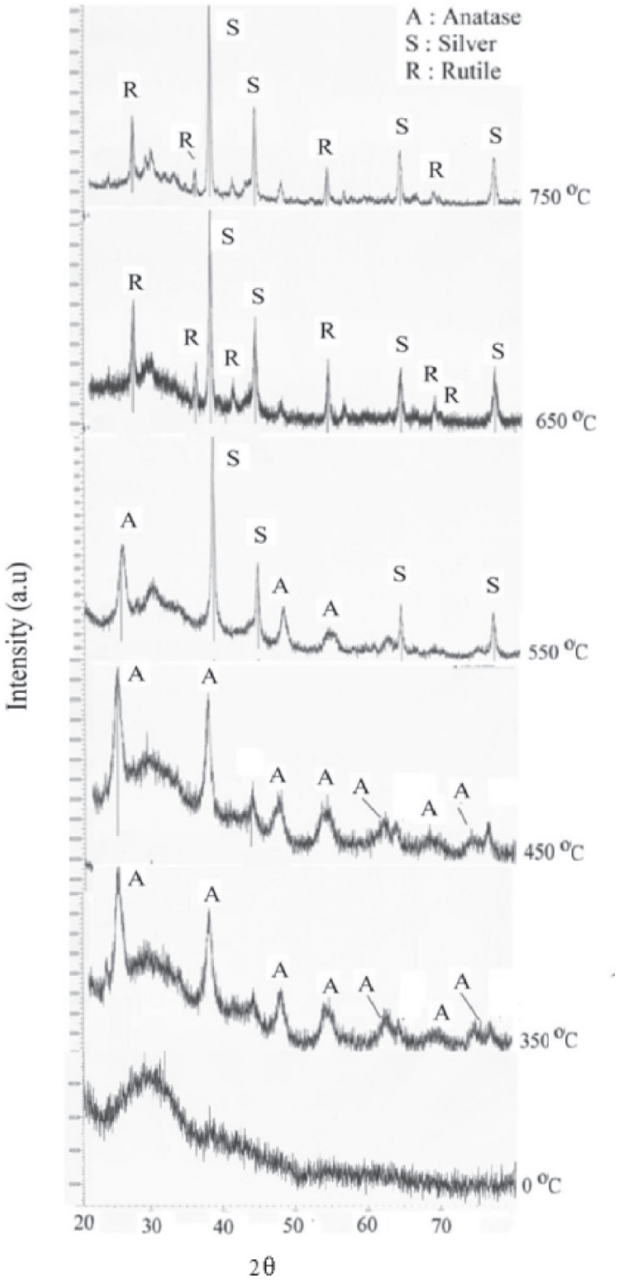

Fig. .2. X-ray diffractrograms of Ag doped TiO_2 catalyst: 0ºC (without calcinations), catalyst calcinated at 350ºC, 450ºC, 550ºC, 650ºC and 750ºC temperatures (Ag-TiO_2 catalyst synthesized through Ist sol gel route and used as mobilized form, A = Anatase, S = Silver).

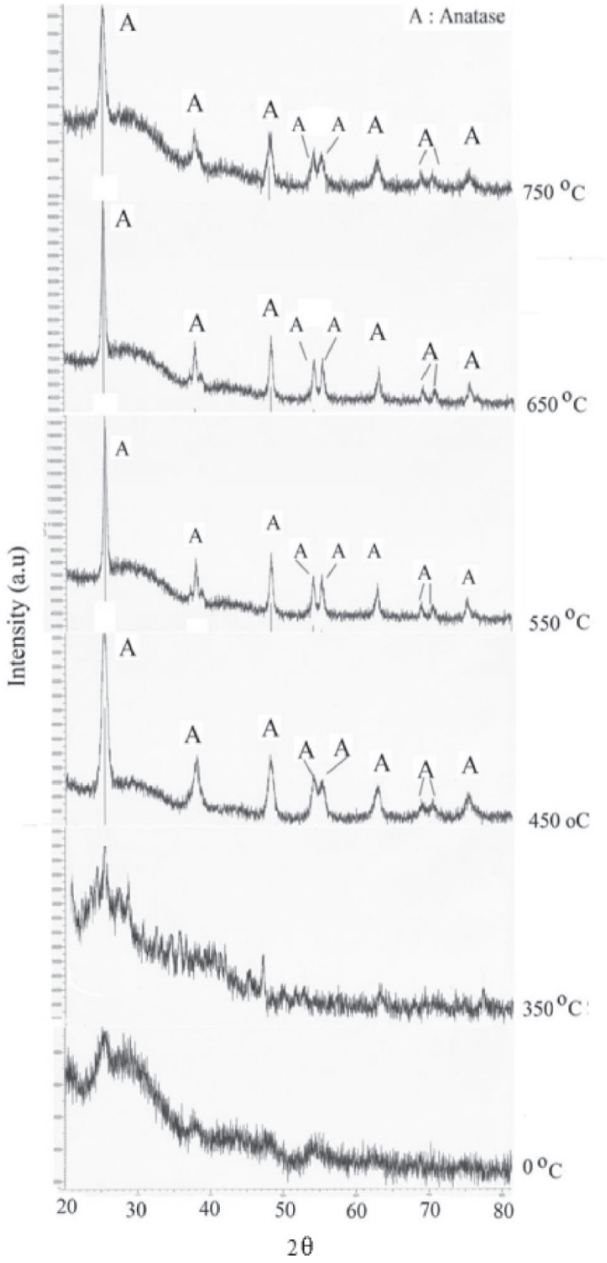

Fig. 3 X-ray diffractrograms of TiO_2 catalyst: 0ºC (without calcination), catalyst calcinated at 350ºC, 450ºC, 550ºC, 650ºC and 750ºC temperatures (TiO_2 catalyst synthesized through second sol gel route and used as immobilized, A = anatase).

of the XRD graphs shown in figures are in agreement with findings reported in the literature, and very well matched with the profile provided by the joint committee on powder diffraction standards.

However, X-ray diffractogram of M1A2, M1A3, and M1A4 (Fig. 1) exhibited strong diffraction corresponding peaks of titanium oxide matched with JCPDS files PDF: 04-0477 (2θ = 25.354, 37.785, 38.507, 53. 922, 55.116, and 62.728), PDF: 86-1157 (25.322, 37.863, 48.064, 53.975, 55.094, and 62.756), and PDF: 86-1157 (25.322, 37.863, 48.064, 53.975, 55.094, 62.756, 70.330, and 75.141), and crystallite phase was confirmed as anatase and lattice structure was tetragonal. The crystal size for the anatase was 9.34 nm, 14.83 nm, and 18.01 nm, and the percent crystal and percent amorphous ratios were 60.4:39.6, 58.8:41.2, and 68.9:31.1, respectively. X-ray diffractrograms illustrate that the anatase phase of TiO_2 is dominating and became sharper as calcination temperatures increased to 550ºC, but going to 650-750ºC rutile phase appeared and few anatase peaks started to degrade/disappear.

X-ray diffractogram of M1B2 calcinated at 350ºC (Fig. 2) indicates corresponding peaks of titanium oxide matched with JCPDS profile PDF: 78-2486

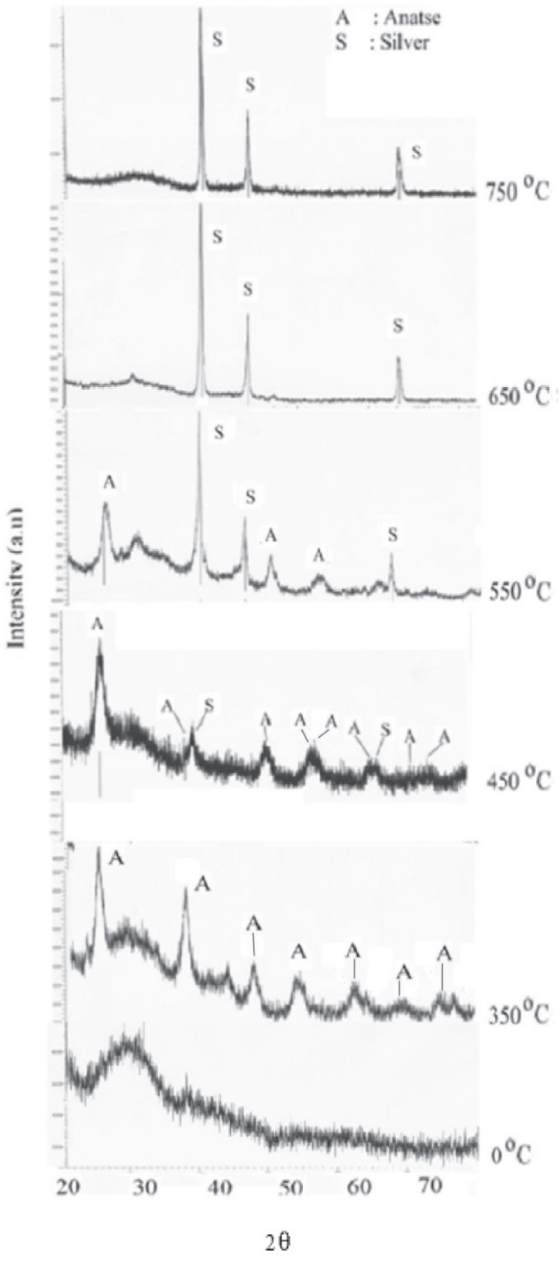

Fig. 4. X-ray diffractograms of Ag doped TiO_2 catalyst: 0ºC (without calcination), catalyst calcinated at 350ºC, 450ºC, 550ºC, 650ºC and 750ºC temperatures (Ag-TiO_2 catalyst synthesized through second sol gel route and used as immobilized, A = Anatase, S = Silver).

(2θ = 25.307, 37.79, 48.043, 55.068, 62.689, 70.298, and 75.05), crystallite phase was anatase, lattice structure was tetragonal, crystal size was 13.82 nm, and the percent crystal and percent amorphous ratio was found to be 50.87:49.24. Catalyst M1B3 calcinated at 450ºC (Fig. 2) showed corresponding peaks of titanium oxide matched with JCPDS profile PDF: 86-1157 (2θ = 25.322, 37.863, 48.064, 53.975, 62.756, 68.870, and 75.141), crystallite phase of composite of anatase, lattice structure of tetragonal. Crystal size of the anatase was found to be 14.6 nm and percent crystal and percent amorphous ratio was found to be 49.7:50.3. Whereas, catalyst M1B4 calcinated at 550ºC (Fig. 2) possessed corresponding peaks of titanium oxide/silver matched with JCPDS profile PDF: 86-1157 (2θ = 25.322, 48.062, 55.094, 62.756, 68.870, and 76.08) PDF: 87-0720 (38.201, 44.402, 64.602, and 77.600), anatase/silver crystals were identified in the catalyst, and latice structure was composite of tetragonal/cubic, crystal size was 23.19 nm, as well as percent crystal and percent amorphous ratio was found to be 59.5:40.5. Silver and TiO_2 composite crystal structure appeared at 550ºC and its catalytic performance also increased (Fig. 5) due to the electron scavenging property of Ag and the reducing band gape energy of TiO_2.

Catalysts M1A5 and M1A6 calcinated at 650ºC and 750ºC (Fig. 1) revealed that as temperature increased to more than 550ºC, the corresponding peaks of titanium oxide crystalites turned to rutile/anatase composite phase and matched with JCPDS profile PDF: 86-1156 (2θ = 25.335, 37.809, 38.611, 53.921, 55.138, 62.753, 68.807, 70.394, and 75.126) and PDF: 86-0148 (2θ = 27.462, 29.228, and 39.228), lattice structure was tetragonal, crystal sizes were 22.39 nm and 29.5 nm, respectively, as well as percent crystal and percent amorphous ratio being found to be 70.4:29.6 and 74.3:25.7, respectively. It is well known that crystal phase transformation from anatase to rutile phase occurs on calcination of TiO_2 at high temperatures [36, 49-51]. Both anatase and rutile phases are highly crystalline in nature, but anatase phase of titanium dioxide (TiO_2) has its unique properties and is more effective in photocatalysis than rutile phase [52]. Catalyst M1B5 calcinated at 650ºC (Fig. 2) possessed corresponding peaks of titanium oxide matched with JCPDS profile PDF: 86-0148 (2θ = 27.445, 36.095, 41.256, 54.342, 56.646, and 69.032), PDF: 01-1167(38.204, 44.370, 64.179, and 77.549), crystalline phase of rutile/silver, and lattice structure of orthormbic/cubic. Crystal size of rutile was 23.09 nm as well as percent crystal and percent amorphous ratio found to be 59.40:40.5. Catalyst M1B6 calcinated at 750ºC (Fig. 2) showed corresponding peaks of titianum oxide/silver, and crystal phase was identified as rutile/silver composite phase matched with JCPDS profile PDF: 86-0148 (2θ = 27.462, 36.127, 54.384, and 69.085), PDF: 87-0720 (2θ = 38.201, 44.402, 64.602, and 77.600), lattice structure was composite of tetragonal/cubic, crystal size of rutile/silver composite catalyst was calculated as 26.32 nm as well as percent crystal and percent amorphous ratio found to be 70.3:29.7. When calcination temperature was increased up to 650ºC and 750ºC as a result of anatase peaks being suppressed (eventually degraded), rutile phase appeared on these calcination temperatures (650ºC and 750ºC) and showed a decrease in photocatalytic performance when used to treat synthetic textile effluent of Remazol red RGB (Fig. 5)

Accordingly, X-ray diffraction patterns of TiO_2 and Ag-doped TiO_2 used in immobilized applications (synthesized through another sol-gel route because

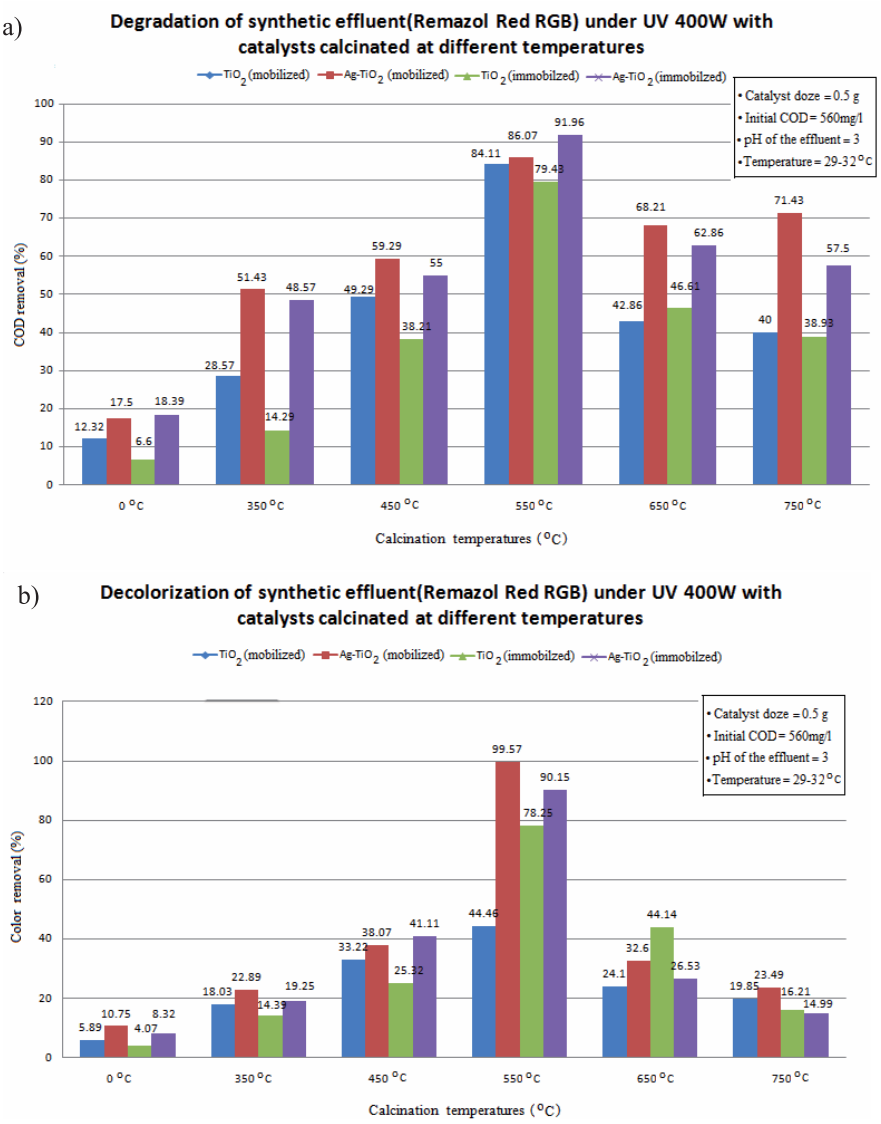

Fig. 5. Photocatalytic degradation and decolorization of synthetic textile effluent with catalysts at 0ºC (without calcination), catalyst calcinated at 350ºC, 450ºC, 550ºC, 650ºC and 750ºC temperatures a) COD removal %. b) Color removal %.

Table 1. X-ray diffrectromtric data of TiO_2 (mobilized) catalyst: 0ºC (without calcination), catalyst calcinated at 350ºC, 450ºC, 550ºC, 650ºC and 750ºC temperatures showing Corresponding Peaks, crystalline phase, structure/lattice, JCPDS, crystal size (nm), % crystal and % amorphous.

Parameters	Catalyst calcinated at different temperatures					
	M1A1	M1A2	M1A3	M1A4	M1A5	M1A6
Calcination temperature (°C)	0	350	450	550	650	750
Correspond peak	NILL	Titanium oxide	Titanium oxide	Titanium oxide	Titanium oxide	Titanium oxide
Cristalite Phase	NILL	Anatase,Syn	Anatase, syn	Anatase, syn	a) Rutile, syn b) Anatase, syn	a) Rutile, syn b) Anatase, syn
Latice/Structure	Amorphous	Tetragonal	Tetragonal	Tetragonal	Tetragonal	Tetragonal
JCPDS	-	PDF. 04-0477	PDF. 86-1157	PDF.86-1157	a) PDF.86-0148 b) PDF.86-1156	a) PDF. 86-0148 b) PDF. 86-1156
Crystal size nm	0	9.34	14.83	18.01	22.39	29.5
% Crystal	0	60.4	58.8	68.9	70.4	74.3
% Amorphous	0	39.6	41.2	31.1	29.6	25.7

Table 2. X-ray diffrectromtric data of Ag-TiO_2 (mobilized) catalyst: 0ºC (without calcination), catalyst calcinated at 350ºC, 450ºC, 550ºC, 650ºC and 750ºC temperatures showing Corresponding Peaks, crystalline phase, structure/lattice, JCPDS, crystal size (nm), % crystal and % amorphous.

Parameters	Catalyst calcinated at different temperatures					
	M1B1	M1B2	M1B3	M1B4	M1B5	M1B6
Calcination temperature (ºC)	0	350	450	550	650	750
Correspond peak	NILL	Titanium oxide	Titanium oxide	a) Titanium oxide b) Silver	a). Titanium oxide b) Silver	a) Titanium oxide b) Silver
Cristalite Phase	NILL	Anatase, syn	a). Anatase, syn	a) Anatase b) Silver	a) Rutile,syn b) Silver	a) Rutile,syn b) Silver
Latice/Structure	Amorphous	Tetragonal	Tetragonal	a) Tetragonal b) cubic	a) Tetragonal b)cubic	a) Tetragonal b) cubic
JCPDS	-	PDF 78-2486	PDF 86-1157	a) PDF 86-1157 b) PDF 87-0720	a) PDF 86-0148 b) PDF 01-1167	a) PDF 86-0148 b) PDF 87-0720
Crystal size nm	0	13.82	14.6	23.19	23.09	26.32
% Crystal	0	50.87	49.7	59.5	59.40	70.3
% Amorphous	0	49.24	50.3	40.5	40.5	29.7

of its performance and better gel adhesion on to the substrate) are shown in Figs 3 and 4. TiO_2 and Ag-doped TiO_2 were coded as M2A1 and M2B1 (pulverized but not calcinated), M2A2 and M2B2 (calcinated at 350ºC), M2A3 and M2B3 (calcinated at 450ºC), M2A4 and M2B4 (calcinated at 550ºC), M2A5 and M2B5 (calcinated at 650ºC), and M2A6 and M2B6 (calcinated at 750ºC).

Table 3 and 4 show the X-ray diffrectromtric data, with results revealing that no obvious diffraction peaks are observed in catalysts M2A1, M2A2, and M2B1 (Figs 3-4), and from this it is inferred that TiO_2 is amorphous.

X-ray diffractogram of M2B2 calcinated at 350ºC (Fig. 2) indicates corresponding peaks of titanium oxide matched with JCPDS profile PDF: 78-2486 (2θ = 25.307, 37.79, 48.043, 55.068, 62.689, 70.298, and 75.05), crystallite phase was anatase, lattice structure was tetragonal, crystal size was 8.39 nm, as well as percent crystal and percent amorphous ratio found to be 52.3:47.7.

Catalysts M2A3, M2A4, M2A5, and M2A6 calcinated at 450ºC, 550ºC, 650ºC, and 750ºC (Fig. 3) possessed corresponding peaks of titanium oxide matched with JCPDS PDF: 86-1157 (2θ = 25.322, 37.863, 48.064, 53.975, 55.094, 62.758, 68.870, 70.330, and 75.141), PDF: 21-1272 (2θ = 25.281, 37.801, 48.050, 53.891, 55.062, 62.690, 68.762, and 70.311), PDF: 86-1156 (2θ = 25.335, 37.809, 48.104, 53.921, 55.138, 62.753, 68.807, and 70.394), and PDF: 86-5117 (2θ = 25.322, 37.863, 48.064, 53.975, 55.094, 62.756, 68.870, 70.330, and 75.141), lattice structure was found as tetragonal, crystallite phase was anatase, crystal size was 11.31 nm,

Table 3. X-ray diffrectromtric data of TiO_2 (immobilized) catalyst: 0ºC (without calcination), catalyst calcinated at 350ºC, 450ºC, 550ºC, 650ºC and 750ºC temperatures showing Corresponding Peaks, crystalline phase, structure/lattice, JCPDS, crystal size (nm), % crystal and % amorphous.

Parameters	Catalyst calcinated at different temperatures					
	M2A1	M2A2	M2A3	M2A4	M2A5	M2A6
Calcination temperature (ºC)	0	350	450	550	650	750
Correspond peak	NILL	NILL	Titanium oxide	Titanium oxide	Titanium oxide	Titanium oxide
Cristalite Phase	NILL	NILL	Anatase, syn	Anatase, syn	Anatase, syn	Anatase, syn
Latice/Structure	Amorphous	Amorphous	Tetragonal	Tetragonal	Tetragonal	Tetragonal
JCPDS	-	-	PDF 86-1157	PDF 21-1272	PDF 86-1156	PDF 86-1157
Crystal size nm	0	0	11.31	13.26	20.53	23.27
% Crystal	0	0	72	58.7	53.5	66.9
% Amorphous	0	0	28	41.3	46.5	33.1

Table 4. X-ray diffrectromtric data of Ag-TiO_2 (immobilized) catalyst: 0ºC (without calcination), catalyst calcinated at 350ºC, 450ºC, 550ºC, 650ºC and 750ºC temperatures showing Corresponding Peaks, crystalline phase, structure/lattice, JCPDS, crystal size (nm), % crystal and % amorphous.

Parameters	Catalyst calcinated at different temperatures					
	M2B1	M2B2	M2B3	M2B4	M2B5	M2B6
Calcination temperature (ºC)	0	350	450	550	650	750
Correspond peak	NILL	Titanium oxide	a) Titanium oxide / b) Silver	a) Titanium oxide / b) Silver	Silver	Silver
Crystalite Phase	NILL	Anatase, syn	a) Anatase, syn b) Silver	a) Anatase, syn b) Silver	Silver	Silver
Latice/Structure	Amorphous	Tetragonal	a) Tetragonal b) Cubic	a) Tetragonal b) Cubic	Cubic	Cubic
JCPDS	-	PDF 78-2486	PDF 01-1167 PDF 01-0562	PDF 86-1157 PDF 87-0720	PDF 87-0720	PDF 87-0720
Crystal size nm	0	8.39	26.31	26.56	26.76	27.50
% Crystal	0	52.30	49.40	65.0	69.9	65.70
% Amorphous	0	47.70	50.60	35.0	30.10	34.30

13.26 nm, 20.53 nm and 23.27 nm, respectively, as well as percent crystal and percent amorphous ratio of 72:28, 58.7:41.3, 53.5:46.3, and 66.9:33.1, respectively.

M2B3 calcinated at 450ºC (Fig. 4) showed corresponding peaks of titanium dioxide matched with JCPDS file PDF: 01-0562 (2θ = 25.282, 37.934, 48.376, 53.888, 55.296, and 62.728) and PDF: 01-1167 (2θ = 38.101, 44.370, and 64.179) and, TiO_2/silver composite crystals were found, crystallite phase of titanium dioxide was anatase, lattice structure was found as tetragonal, crystal size was 26.31 nm, as well as percent crystal and percent amorphous ratio was 49.40:50.60.

Whereas, X-ray diffractograms of M2B4 calcinated at 550ºC (Fig. 4) possessed corresponding peaks of silver matched with JCPDS profile PDF: 86-1157 (2θ = 25.322, 48.062, 55.094, 62.756, 68.870, and 76.08) and PDF: 87-0720 (2θ= 38.201, 44.402, 64.602), titanium oxide/silver composite crystals were identified, crystallite phase was anatase, lattice structure was composite of tetragonal/ cubic, crystal size was 26.56 nm, as well as percent crystal and percent amorphous ratio found as 65.0:35.0.

M2B5 and M2B6 (Fig. 4) showed that silver was identified in corresponding peaks and matched with JCPDS profile PDF: 87-0720 (2θ =38.201, 44.402, and 64.602) and PDF: 87-0720 (2θ = 38.201, 44.402, and 64.602), lattice structure of silver identified as cubic, crystal size were 26.76 nm and 27.5 nm, respectively, as well as percent crystal and percent amorphous ratio found to be 69.9:30.10 and 65.7:34.30, respectively. At 550ºC calcinations temperature silver and TiO_2 composite catalyst structure formed and gave optimum photcatalytic performance (Fig. 5), but as calcinations increased up to 650ºC and 750ºC anatase peaks disappeared due to phase change to rutile at high temperature, but X-ray diffractrogram showed only silver crystals because they grow in size with temperature and rutile crystals were suppressed.

Table 5. Characteristics of synthetic textile effluent (Remazol Red RGB).

Parameter	Value
pH Initial dye conc.	3 10 ppm
COD (mg/L)	560
Absorbance ($A_{519\ nm}$)	1.647

Photocatalytic Activity of TiO_2 and Ag- TiO_2

The effect of calcination temperatures (350ºC, 450ºC, 550ºC, 650ºC, and 750ºC) on the performance of TiO_2 and Ag-TiO_2 catalysts was evaluated in terms of percentage removal of chemical oxygen demand (COD) and removal of colour of synthetic textile effluent (remazol red RGB) in a double-walled rectangular box reactor. Standard procedures given in "Standard methods were followed for the examination of water and wastewater" [53].

Photocatalytic activity of the catalysts was evaluated through degradation of a 1 litre sample of synthetic effluent (remazol red RGB) with initial dye concentration of 10 ppm, intial COD 560mg/l, pH of the effluent was adjusted at 3 as pH was optimized, and results are reported in our previous paper [46]. Photocataytic degradation was carried out under UV (400W) radiation.

Table 6 shows the results of maximum degradation and decolourization (COD removal percentage and color removal percentage), observed with the catalysts

Table 6. COD removal (%) and Colour removal (%) of the synthetic effluent (catalyst dose 0.5 g and 60 min irradiation time) degraded with catalysts 0ºC (without calcinations) and calcinated at 350ºC, 450ºC, 550ºC, 650ºC and 750ºC temperatures.

Sr. No	Catalysts	COD and Color removal (%) of synthetic textile effluent											
		0°C		350°C		450°C		550°C		650°C		750 °C	
		COD	Color	COD	Color	COD	Color	COD	Color	COD	Color	COD	Color
1	TiO_2 (mobilized)	12.32	5.89	28.57	18.03	49.29	33.22	84.11	44.46	42.86	24.10	40.0	19.85
2	Ag-TiO_2 (mobilized)	17.5	10.75	51.43	22.89	59.29	38.07	86.07	99.57	68.21	32.60	71.43	23.49
3	TiO_2 (immobilized)	6.6	4.07	14.29	14.39	38.21	25.32	79.43	78.25	46.61	44.14	38.93	16.21
4	Ag-TiO_2 (immobilized)	18.39	8.32	48.57	19.25	55	41.11	91.96	90.15	62.86	26.53	57.50	14.99

Table 7. Statistical Descriptive analysis: value of mean (M) and standard deviation (SD) of factors "calcinations temperature" as catalyst was calcinated at different temperatures and labelled in SPSS software as catalysts 0ºC = 1 (without calcinations) and calcinated at 350ºC = 2, 450ºC = 3, 550ºC = 4, 650ºC and 750ºC = 5 temperatures.

Parameters	Mean (M) n = 24	Standard Deviation (SD) n = 24
Calcination temperature	3.5	1.74

calcinated at 550ºC. It is observed that with increased calcination of the catalysts up to a certain temperature increases its photcatalytic activity.

TiO_2 (mobilized), Ag-TiO_2 (mobilized), TiO_2 (immobilzed), and Ag-TiO_2 (immobilzed) calcinated at 550ºC showed maximum performance at optimum treatment conditions (UV-400W radiataion, volume of the effluent 1 litre, catalyst load 0.5 gram, catalyst mesh (with four layers coating of TiO_2 and Ag-TiO_2), pH of effluent 3, intial COD 560 mg/l, and temperature was maintained ranging between 29-32ºC during treatment).

Results shown in Table 6 and Fig. 5(a-b) illustrate that the obtained percentage removal of COD (color) values were 84.11% (44.46%), 86.07% (99.57%), and 79.43% (78.25%), 91.96% (90.15%) for TiO_2 (mobilized), Ag-TiO_2(mobilized), TiO_2 (immobilzed), and Ag-TiO_2 (immobilzed), respectively. Results also revealed that Ag-TiO_2 doped catalysts showed much better results among the rest of the catalysts as shown in Fig. 5(a-b).

Fig. 5 represents COD and color removal percentage of synthetic textile effluent photocatalytic system. Results of photocatalytic degradation of the synthetic textile effluent (remazol red RGB) with initial dye concentration of 10 ppm, COD concentration of 560 mg/l, at pH 3 revealed that catalysts calcinated at different temperatures performed differently during the degradation and decolorization process (Table 6, Fig. 5). At calcination temperature of 350ºC all catalysts showed low catalytic degradation as well as low decolourzation, which is evidence of low catalytic activity, except the catalyst calcinates at 550ºC. It is also revealed that along with increasing the calcination temperature, catalytic activity increased until 550ºC, at which point the highest photocatalytic activity is observed. Furthermore, catalysts calcinated at 650ºC and 750ºC didn't show

Table 8. One-way ANOVA results of COD removal and color removal percentage with respect to the factor "Calcination temperature".

Variables	Calcination Temperature						
		Sum of Squares	Df	Mean Square	*F*	Sig. (P<0.05)	Decision
COD removal %	Between Groups	11179.575	5	2235.915	15.981	.000	Significant mean difference
	Within Groups	2518.420	18	139.912			
	Total	13697.996	23				
Color removal %	Between Groups	12398.186	5	2479.637	20.046	.000	Significant mean difference
	Within Groups	2226.575	18	123.699			
	Total	14624.761	23				

Table 9. The results of the Tukey post hoc tests (multiple comparison) dependent variable: COD % removal (Tukey HSD).

Sr. No.	Significance Mean difference between the Groups	*p<0.05*
1	0ºC VS 450ºC	0.004
2	0ºC VS 550ºC	0.000
3	0ºC VS 650ºC	0.001
4	0ºC VS 750ºC	0.003
5	550ºC VS 0ºC	0.000
6	550ºC VS 350ºC	0.000
7	550ºC VS 450ºC	0.006
8	550ºC VS 650ºC	0.021
9	550ºC VS 750ºC	0.009

Table 10. The results of the Tukey post hoc tests (multiple comparison) dependent variable: Color removal percentage (Tukey HSD).

Sr. No.	Significance Mean difference between the Groups	*p<0.05*
1	0ºC VS 450ºC	0.029
2	0ºC VS 550ºC	0.000
3	550ºC VS 0ºC	0.000
3	550ºC VS 350ºC	0.000
4	550ºC VS 450ºC	0.000
5	550ºC VS 650ºC	0.000
6	550ºC VS 750ºC	0.000

much increase in percentage removal in degradation and decolourization. Results from Table 1-4 and Figs 1-4 also reveled that at 550ºC calcinations temperature anatase crystalline phase is dominating and crystaline size increased slowly as a result of performance of the catalysts proven to be in favor of photocatalytic degradation and decolourization of the synthetic effluent shown in Table 6 and Fig. 5(a-b).

Results of XRD patterns give evidence that anatase crystal phase of TiO_2 was obtained at 550ºC calcination temperature. We concluded that the higher photocatalytic activity of TiO_2 is due to the parameter of calcination temperature to obtain the required crystalline phase. Photocatalytic activity was obtained better in the anatase phase of TiO_2 for the degradation of all substances as compared with the rutile phase. Photocatalytic degradation of dyes and organic contaminants in water using nanocrystalline anatase and rutile TiO_2 [54].

The activity of TiO_2 and Ag-TiO_2 highly depends on its crystal phase. The particle size of the catalyst also plays a very important role in its photocatalytic activity. A decrease in particle size results in large surface area, which is favorable for high photocatalytic activity. Based on XRD data and performance in photocatalytic activity of catalysts it is revealed that a calcination temperature of 550ºC with small crystal size is most effective.

Statistical Analysis

The descriptive analysis of the results was carried out through SPSS (V15) in terms of mean, standard deviation, analysis of variance (ANOVA). Statistical correlations between groups were calculated using one-way ANOVA. According to the descriptive analysis, the mean and standard deviation values for the parameter "calcination temperature" are M = 3.5 and SD = 1.74, respectively. The values of calcination temperature mean = 3.5 indicates that results of the treatment are in favour of the catalyst calcinated at 550ºC, as well as the SD = 1.74 indicating that the overall treatment results obtained by using catalyst calcinated at 550ºC are not scattered (Table 7).

Analysis of variance (ANOVA) with F values of 95% significance level ($\alpha = 0.05$) is used to statistically evaluate the experimental data of chemical oxygen demand (COD) and color removal percentage. Analysis revealed that catalyst calcinaed at 550ºC showed optimum results for degradation and decolourization of synthetic effluent (remazol red RGB). Results were compared through one-way ANOVA tests (Statistics 15; SPSS Inc. Package) (Table 7). According to the results, there was a significant effect of "calcination temperature" ($p<0.05$) as p-value is 0.000 (F = 15.981) on degradation and decolourization of the effluent, which is less than the significance level of 0.05 (Table 8). These values indicate that there is a significance mean difference between the COD removal percentage values when considering the parameter of the calcination temperatures (0ºC, 350ºC, 450ºC, 550ºC, 650ºC, and 750ºC (Table 8). Thus, a post hoc test reveals that the significance difference found at the level $p<0.05$ in the results of the COD removal and color removal percentage obtained when synthetic effluent was treated with the catalysts calcinated at 0ºC and 550ºC (Table 9 and 10).

Significant mean values are mentioned in Table 9, which are less than the level of significance ($p<0.05$), which shows that there is a major difference present in the results of COD removal percentage between 0ºC ($p<0.05$) VS 450ºC, 550ºC, 650ºC, and 750ºC. As well as between 550ºC ($p<0.05$) VS 0ºC, 350ºC, 450ºC, 550ºC, 650ºC, and 750ºC. We also found that there is a large significant mean difference found between 0ºC ($p<0.05$) VS 550ºC ($p<0.05$) for the results of COD removal percentage. This indicates that optimum COD removal percentage was achieved with catalyst calcinated at 550ºC.

Results of color removal percentage are shown in Table 10. We found that values of color removal percentage obtained from the treatment carried out using

catalysts calcinated at 0ºC ($p<0.05$) have significant mean difference with the results obtained from catalysts calcinated at 450ºC and 550ºC. There is also another difference found between values of color removal percentage in the catalyst calcinated at 550ºC ($p<0.05$) VS 0ºC, 350ºC, 450ºC, 550ºC, 650ºC, and 750ºC. From Table 10 we infer that a major difference in the results of color removal percentage is achieved between 0ºC VS 550ºC, which indicates that optimum colour removal percentage was achieved by using catalyst calcinated at 550ºC.

Conclusions

The higher photocatalytic activity of TiO_2 is due to the parameter of calcination temperature to obtain the required crystalline phase. Photocatalytic activity was obtained better in anatase phase of TiO_2 for the degradation of all substances as compared with rutile phase. Results have given evidence that anatase crystal phase of TiO_2 was obtained at 550ºC calcination temperature. The activity of TiO_2 and Ag-TiO_2 highly depends on its crystal phase. The particle size of the catalyst also plays a very important role in its photocatalytic activity as small particle size results in large surface area, which is favorable for high photocatalytic activity. Based on XRD data and performance in photocatalytic activity of catalysts, it is revealed that calcination temperatures of 550ºC with small crystal size are most effective. TiO_2 and Ag-doped TiO_2 proved to be very effective catalysts in photocatlytic degradation of synthetic textile effluent. The photocatalytic activity of catalysts found in results with respect to their calcination temperatures can be stated in the following order: 550°C > 450°C > 650°C > 750°C >350°C > 0°C. Moreover, maximum photocatalytic activity was achieved by catalysts calcinated at 550°C as 91.96% degradation (COD removal percentage) with Ag-doped TiO_2 immobilized catalyst and 99.57% decolorization (colour removal percentage) was achieved with Ag-doped TiO_2 mobilized catalyst on 60 min treatment of synthetic textile effluent (Remazol red RGB: 10 ppm concentration, pH3). This is because of the presence of Ag doping and anatase crystalline phase of TiO_2, which favored degradation and decolourization. The order of degradation and decolourization at 550°C found out as Ag-TiO_2 (immobilized) > Ag-TiO_2 (mobilized) > TiO_2 (mobilized) > TiO_2 (immobilized) and Ag-TiO_2 (mobilized) >Ag-TiO_2(immobilised)> TiO_2 (immobilized) > TiO_2 (mobilized), respectively.

Acknowledgements

The authors extend their sincere thanks to the Centre of Excellence in Solid State Physics, University of the Punjab, Lahore for XRD analysis of the catalyst samples for this research.

Conflict of Interest

The authors declare no conflict of interest.

Refrences

1. AKRAM T.M., AHMAD N., SHAIKH I.A. Photocatalytic degradation of synthetic textile effluent by modified sol-gel, synthesized mobilized and immobilized TiO_2, and Ag-doped TiO_2. Polish Journal of Environmental Studies, **25** (4), **2016**.
2. VILLEGAS-NAVARRO A., RAMIREZ M.Y., SALVADOR M.S.S.B., GALLARDO J.M. Determination of wastewater LC50 of the different process stages of the textile industry, Ecotoxicology Environmental Safety, **48** (1), 56, **2001.**
3. MERIÇ S., SELCUK H., BELGIORNO V. Acute toxicity removal in textile finishing wastewater by Fenton's oxidation, ozone and coagulation-flocculation processes, Water Research, **39** (6), 1147, **2005**.
4. SHARMA K.P., SHARMA S., SINGH P., KUMAR S., GROVER R., SHARMA P.K. A comparative study on characterization of textile wastewaters (untreated and treated) toxicity by chemical and biological tests, Chemosphere, **69** (1), 48, **2007**.
5. GÜMÜŞ D., AKBAL F. Photocatalytic degradation of textile dye and wastewater. Water, air, and soil pollution, **216** (1-4), 117, **2011**.
6. KHAN S., MALIK A. Environmental and health effects of textile industry wastewater, Environmental deterioration and human health, 55, **2014**.
7. KULKARNI M., THAKUR, P. photocatalytic degradation of real textile industrial effluent under uv light catalyzed by metal oxide nanoparticles. Nepal Journal of Science and Technology, **15** (2), 105, **2015**.
8. MONDAL C., BHAGCHANDANI G. Novel effluent treatment technique in textile industry, International journal of advance research and innovative ideas in education , **2** (3), 2395, **2016**.
9. ALATON I.A., BALCIOGLU I.A., BAHNEMANN D.W. Advanced oxidation of a reactive dyebath effluent: comparison of O_3, H_2O_2/UV-C and TiO_2/UV-A processes. Water Research, **36** (5), 1143, **2002**.
10. PAMECHA K., MEHTA V. KABRA B.V. photocatalytic degradation of commercial textile azo dye reactive blue 160 by heterogeneous Photocatalysis, **7** (3), 95, **2016**.
11. DE MORAES S.G., FREIRE R.S., DURAN N. Degradation and toxicity reduction of textile effluent by combined photocatalytic and ozonation processes. Chemosphere, **40** (4), 369, **2000**.
12. MAHMOODI N.M., ARAMI M., LIMAEE N.Y., GHARANJIG K., ARDEJANI F.D. Decolorization and mineralization of textile dyes at solution bulk by heterogeneous nanophotocatalysis using immobilized nanoparticles of titanium dioxide. Colloids and Surfaces A: Physicochemical and Engineering Aspects, **290** (1), 125, **2006**.
13. PEKAKIS P.A., XEKOUKOULOTAKIS N.P., MANTZAVINOS D. Treatment of textile dyehouse wastewater by TiO_2 photocatalysis. Water research, **40** (6), 1276, **2006**.
14. MARTINS A.F. WILDE M.L., DA SILVEIRA C. Photocatalytic degradation of Brilliant Red dye and textile

wastewater, Journal of Environmental Science and Health, Part A: Toxic/Hazardous Substances and Environmental Engineering, **41** (4), 675, **2006**.
15. ALINSAFI A., EVENOU F., ABDULKARIM E.M., PONS M.N., ZAHRAA O., BENHAMMOU A., YAACOUBI A., NEJMEDDINE A. Treatment of textile industry wastewater by supported photocatalysis, Dyes and Pigments, **74** (2), 439, **2007**.
16. PARK H., KIM H.I., MOON G.H., CHOI W. Photoinduced charge transfer processes in solar photocatalysis based on modified TiO_2. Energy & Environmental Science, **9** (2), 411, **2016**.
17. POKHARNA S., SHRIVASTAVA R. Photocatalytic treatment of textile industry effluent using titanium oxide. Int. J. Recent Res. Rev, 2, 9, **2013**.
18. LIMA C.S., BATISTA K.A., RODRÍGUEZ A.G., SOUZA J.R., FERNANDES K.F. Photodecomposition and color removal of a real sample of textile wastewater using heterogeneous photocatalysis with polypyrrole, Solar Energy, **114**, 105, **2015**.
19. XIAOBO C. SAMUEL S.M. Titanium dioxide nanomaterials: synthesis, properties, modifications, and applications. Chem. Rev. **107** (7), 2891, **2007**.
20. YU J., JARONIEC M., YU H., FAN W. Synthesis, characterization, properties, and applications of nanosized photocatalytic materials. Journal of Nanomaterials. Article ID 783686, **3** (17), **2012**.
21. SAMIRA S. Photocatalytic Degradation of Crystal Violet (CI Basic Violet 3) on Nano TiO_2 Containing Anatase and Rutile Phases (3: 1). Journal of Thermodynamics & Catalysis, 2012, **2013**.
22. BAGHERI S., RAMIMOGHADAM D., YOUSEFI A. T., HAMID S.B.A. Synthesis, Characterization and Electrocatalytic Activity of Silver Doped-Titanium Dioxide Nanoparticles. Int. J. Electrochem. Sci, 10, 3088, **2015**.
23. PHOOHINKONG W., MEKPRASART W., PECHARAPA W. Photocatalytic performance of Anatase/Rutile TiO_2 composite against different organic dyes, Journal of Science and Technology, **8** (1), 170, **2016**.
24. LI Y., XU H., OUYANG S., YE J. Metal – organic frameworks for photocatalysis. Physical Chemistry Chemical Physics, **18** (11), 7563, **2016**.
25. IBRAHIM S.A., SREEKANTAN S. Effect of pH on TiO_2 nanoparticles via sol-gel method. Advanced Materials Research, **173**, 184, **2011**.
26. KAUR R., PAL B. Co-catalysis effect of different morphological facets of as prepared Ag nanostructures for the photocatalytic oxidation reaction by Ag-TiO_2 aqueous slurry. Materials Chemistry and Physics, **143** (1), 393, **2013**.
27. YUDOYONO G., ZHARVAN V., ICHZAN N., DANIYATI R., INDARTO B., PRAMONO Y.H., MOCHAMAD Z., DARMINTO. Influence of pH on the formulation of TiO_2 powder prepared by co-precipitation of TiCl3 and photocatalytic activity. In A. Purwanto, A. Nur, & F. Rahmawati (Eds.), AIP Conference Proceedings (Vol. 1710, No. 1, p. 030011). AIP Publishing, **2016**.
28. DEVI G.S., KUMAR K.S., REDDY K.S. Effect of pH on Synthesis of Single-Phase Titania (TiO_2) Nanoparticles and its Characterization. Particulate Science and Technology, **33** (3), 219, **2015.**
29. GRIBB A.A., AND BANFIELD F.J. Particle size effects on transformation kinetics and phase stability in nanocrystalline TiO_2, American Mineralogist, **82**, 717, **1997**.
30. LI B.R., WANG X.H., YAN M., LI L.T. Preparation and characterization of nano-TiO_2 powder. Engineering Materials **224**, 577, **2002**.
31. MEHRIZAD A., GHARBANI P., TABATABII M.S. Synthesis of nanosized TiO_2 powder by sol-gel method in acidic conditions, Journal of the Iranian Chemical Research, **2**, 145, **2009**.
32. MAEDA K., DOMEN K. Photocatalytic water splitting: recent progress and future challenges. The Journal of Physical Chemistry Letters, **1** (18), 2655, **2010**.
33. MUNUSAMY S., SAI R. AXMI APARNA A., PRASAD G.S.V.R. Photocatalytic effect of TiO_2 and the effect of dopants on degradation of brilliant green, Sustainable chemical processes, **1**, 4, **2013**.
34. MUURONEN M., PARKER S.M., BERARDO E., LE A., ZWIJNENBURG M.A., FURCHE F. Mechanism of photocatalytic water oxidation on small TiO_2 nanoparticles. Chemical Science, **2017**.
35. WANG G., XU L., ZHANG J., YIN T., HAN D. Enhanced photocatalytic activity of powders (P25) via calcination treatment. International Journal of Photoenergy, **2012**.
36. CAI J., XIN W., LIU G., LIN D., ZHU D. Effect of calcination temperature on structural properties and photocatalytic activity of Mn-C-codoped TiO_2, Materials Research, **19** (20), 4, **2016**.
37. LEE D.K., KIM S.C., CHO I.C., KIM S.J., KIM S.W. Photocatalytic oxidation of microcystin-LR in a fluidized bed reactor having TiO_2-coated activated carbon. Sep. Purif. Technol. **34**, 59, **2004**.
38. SABRY R.S., AL-HAIDARIE Y.K., KUDHIER M.A. Synthesis and photocatalytic activity of TiO_2 nanoparticles prepared by sol-gel method. Journal of Sol-Gel Science and Technology, **78** (2), 299, **2016**.
39. CARRERA-LÓPEZ R. Effect of the phase composition and crystallite size of sol-gel TiO_2 nanoparticles on the acetaldehyde photodecomposition. Superficies y Vacío, **25** (2), 82, **2012**.
40. JARAMILLO J., GARZÓN B.A., MEJÍA L.T. Influence of the pH of the synthesis using sol-gel method on the structural and optical properties of TiO_2. Journal of Physics: Conference Series, **687** (1), 012099, **2016**.
41. KOKILA P., RAMESHBABU M., SENTHILKUMAR V. Effects of Calcination Temperature, pH and Irradiation time on Photocatalytic Activity of Pure and Doped Titanium Dioxide Nanopowders , International Journal of Modern Science and Technology, **1** (7), 250, **2016**.
42. WANG Q., JIANG Z., WANG Y., CHEN D., YANG D. Photocatalytic properties of porous C-doped TiO_2 and Ag/C-doped TiO_2 nanomaterials by eggshell membrane templating. J. Nanopart. Res., **11**, 375, **2009**.
43. SU C., HONG B.Y., TSENG C.M. Sol-Gel Preparation and Photocatalysis of Titanium Dioxide. Catalysis Today, **96**, 119, **2004**.
44. SEERY K.S., GEORGE R., FLORIS P., PILLAI S.C. Silver doped titanium dioxide nanomaterials for enhanced visible light photocatalysis. J. Photochem. Photobiol. A: Chem., **189**, 258, **2007**.
45. NEPPOLIAN B., EDDY D.R.. SAKAI S., OKADA Y., NISHIJIMA H., ANPO M. Preparation of TiO_2 nano-particle photocatalysts by a multi-gelation method: the effect of pH change, Research on Chemical Intermediates, **34** (1), 103, **2008**.
46. HENDRIX Y., LAZARO A., YU Q., BROUWERS J. Titania-Silica Composites: A review on the photocatalytic activity and synthesis methods, World Journal of Nano Science and Engineering, **5**, 161, **2015**.

47. MARATHE S.D., SHRIVASTAVA S.V. Synthesis of nano sized TiO_2 and its application in photocatalytic removal of methylene blue, Pelagia research library advances in applied science research, **4** (6), 212, **2013**.
48. CARNEIRO J.T., SAVENIJE T.J., MOULIJN J.A., MUL G. Toward a physically sound structure − activity relationship of TiO_2-based photocatalysts. The Journal of Physical Chemistry C, **114**(1), 327, **2009**.
49. AHMADI M., GHASEMI M.R., RAFSANJANI H.H. Study of different parameters in TiO_2 nanoparticles formation. Journal of Materials Science and Engineering, **5** (1), 87, **2011**.
50. YU J-G., HUO-GEN YU, H-G., CHENG B., ZHAO X-J., YU C.J., HO W-K. the effect of calcination temperature on the surface microstructure and photocatalytic activity of TiO_2 thin films prepared by liquid phase deposition, J. Phys. Chem. B, **107** (50), 13871, **2003**.
51. WETCHAKUN N., INCESSUNGVORN B., WETCHAKUN K., PHANICHPHANT S. Influence of calcination temperature on anatase to rutile phase transformation in TiO_2 nanoparticles synthesized by the modified sol-gel method, Materials Letters, **82**, 195, **2012**.
52. CHEN Y.F., LEE C.Y., YENG M.Y., CHIU H.T. The effect of calcination temperature on the crystallinity of TiO_2 nanopowders. Journal of crystal growth, **247** (3), 363, **2003**.
53. APHA. Standard Methods for the examination of water and wastewater. American Public Health Association (APHA), Washington D.C., 20th Edition, **1998**.
54. TAYADE R.J., SUROLIA P.K., KULKARNI R.G., JASRA R.V. Photocatalytic degradation of dyes and organic contaminants in water using nanocrystalline anatase and rutile TiO_2. Science and Technology of Advanced Materials, **8**(6), 455, **2007**.